

GA-A27910

# THE SINGLE-DOMINANT MODE PICTURE OF NON-AXISYMMETRIC FIELD SENSITIVITY AND ITS IMPLICATIONS FOR ITER GEOMETRIC TOLERANCES

by

C. PAZ-SOLDAN, K.H. BURRELL, R.J. BUTTERY, J.S. DEGRASSIE, N.M. FERRARO,  
A.M. GAROFALO, J.M. HANSON, J.D. KING, R.J. LA HAYE, M.J. LANCTOT, N.C. LOGAN,  
P. MARTIN, R. NAZIKIAN, J.-K. PARK, C. PIRON, D. SHIRAKI, W.M. SOLOMON,  
E.J. STRAIT, AND B.J. TOBIAS

SEPTEMBER 2014



## **DISCLAIMER**

This report was prepared as an account of work sponsored by an agency of the United States Government. Neither the United States Government nor any agency thereof, nor any of their employees, makes any warranty, express or implied, or assumes any legal liability or responsibility for the accuracy, completeness, or usefulness of any information, apparatus, product, or process disclosed, or represents that its use would not infringe privately owned rights. Reference herein to any specific commercial product, process, or service by trade name, trademark, manufacturer, or otherwise, does not necessarily constitute or imply its endorsement, recommendation, or favoring by the United States Government or any agency thereof. The views and opinions of authors expressed herein do not necessarily state or reflect those of the United States Government or any agency thereof.

# THE SINGLE-DOMINANT MODE PICTURE OF NON-AXISYMMETRIC FIELD SENSITIVITY AND ITS IMPLICATIONS FOR ITER GEOMETRIC TOLERANCES

by

C. PAZ-SOLDAN<sup>1</sup>, K.H. BURRELL<sup>1</sup>, R.J. BUTTERY<sup>1</sup>, J.S. DEGRASSIE<sup>1</sup>, N.M. FERRARO<sup>1</sup>,  
A.M. GAROFALO<sup>1</sup>, J.M. HANSON<sup>3</sup>, J.D. KING<sup>1</sup>, R.J. LA HAYE<sup>1</sup>, M.J. LANCTOT<sup>1</sup>,  
N.C. LOGAN<sup>2</sup>, P. MARTIN<sup>5</sup>, R. NAZIKIAN<sup>2</sup>, J.-K. PARK<sup>2</sup>, C. PIRON<sup>5</sup>, D. SHIRAKI<sup>4</sup>,  
W.M. SOLOMON<sup>2</sup>, E.J. STRAIT<sup>1</sup>, AND B.J. TOBIAS<sup>2</sup>

This is a preprint of the synopsis for a paper to be  
presented at the Twenty-Fifth IAEA Fusion Energy  
Conf., October 13-18, 2014 in Saint Petersburg,  
Russia.

<sup>1</sup>General Atomics, P.O. Box 85608, San Diego, California, USA

<sup>2</sup>Princeton Plasma Physics Laboratory, Princeton, New Jersey, USA

<sup>3</sup>Columbia University, New York, New York, USA

<sup>4</sup>Oak Ridge National Laboratory, Oak Ridge, Tennessee, USA

<sup>5</sup>Consorzio RFX, Corso Stati Uniti 4, 35127, Padova, Italy

Work supported in part by  
the U.S. Department of Energy under  
DE-FC02-04ER54698, DE-AC02-09CH11466, DE-FG02-04ER54761,  
and DE-AC05-00OR22725

GENERAL ATOMICS PROJECT 30200  
SEPTEMBER 2014





## The single-dominant mode picture of non-axisymmetric field sensitivity and its implications for ITER geometric tolerances

C. Paz-Soldan 1), K.H. Burrell 1), R.J. Buttery 1), J.S. deGrassie 1), N.M. Ferraro 1), A.M. Garofalo 1), J.M. Hanson 2), J.D. King 1), R.J. La Haye 1), M.J. Lanctot 1), N.C. Logan 2) P. Martin 5), R. Nazikian 2), J-K. Park 2), C. Piron 5) D. Shiraki 4), W.M. Solomon 2), E.J. Strait 1), and B.J. Tobias 2)

- 1) General Atomics, San Diego, California 92121, USA
- 2) Princeton Plasma Physics Laboratory, PO Box 451, Princeton, NJ 08543-0451, USA.
- 3) Columbia University, New York, New York 10027, USA.
- 4) Oak Ridge National Laboratory, Oak Ridge, TN, USA.
- 5) Consorzio RFX, Corso Stati Uniti 4, 35127, Padova, Italy.

e-mail contact of main author: paz-soldan@fusion.gat.com

**Abstract.** Experiments at DIII-D have demonstrated that several key  $n=1$  field sensitivities are directly related to their coupling to the least-stable ('dominant') mode of the plasma, and concomitantly that the plasma is remarkably insensitive to  $n=1$  fields which have no net coupling to this single dominant mode. Specifically, plasma rotation and error field (EF) penetration thresholds are nearly unchanged despite application of large amplitude probing fields with no dominant mode coupling, and are thus 'orthogonal' to the dominant mode. The plasma sensitivity to  $n=1$  orthogonal fields is of critical importance as this sets the true geometric tolerance of the tokamak so long as it is equipped with at least a single row of EF correction coils (EFCCs) and its intrinsic 3D field sources are well characterized, thus allowing the coupling of the intrinsic EF to be nulled by the EFCCs. The observed weak sensitivity to the orthogonal field challenges the stringent tolerance requirements currently enforced, as a strong performance recovery when using EFCCs is expected though it is not presently taken into account. In contrast,  $n=2$  fields are found to potentially drive rotation braking despite not coupling to the  $n=2$  dominant mode.

### 1. Introduction and motivation

Recent theoretical advances in understanding the plasma response to non-axisymmetric fields have shown that the plasma response can be represented as a hierarchy of stable modes, found through singular value decomposition[1, 3]. Each mode is orthogonal to one another, and strong (order of magnitude) separation of singular values is usually found. The strong singular value separation implies that the secondary modes can be ignored, effectively rendering the plasma sensitive only to the degree of coupling to the least-stable mode, which is a scalar property of an applied 3D spectrum.

This concept has important consequences for the geometric tolerance of future tokamaks. For tokamaks equipped with at least one row of error field correction coils (EFCCs), these coils can be used to perfectly null the coupling of the intrinsic EF to the same dominant mode. Thus, for plasmas sensitive to only one mode, a complete performance recovery is expected since deleterious coupling is nulled. Furthermore, the magnitude of the intrinsic EF is unimportant, provided the EFCCs have sufficient current capability to null the coupling. If the magnitude of the EF is unimportant, than any geometric tolerance constraints from EF-based limits can be significantly relaxed. Another consequence of the single-mode model is that EFC performed with ex-vessel EFCCs should be as effective as EFC with in-vessel EFCCs, since both couple to the dominant mode.

The applicability of this picture to 3D sensitivity on DIII-D is tested in a variety of scenarios by applying probing fields which are computed to have no net coupling (and are thus ‘orthogonal’) to the least-stable mode. These probing fields simulate the situation in which a large intrinsic EF is present, but has been well corrected, yielding a large residual field with no net coupling.

This work will show that for  $n=1$  fields, the plasma has very weak sensitivity to the orthogonal field, thus validating the single-dominant mode picture.[4] In low density Ohmic scenarios, the  $n=1$  orthogonal field is found to not change EF penetration thresholds. In low  $q_{95}$  L-mode and co-rotating H-mode scenarios, the  $n=1$  orthogonal field is not found to drive significant rotation braking. In all scenarios, the orthogonal field is applied to very large amplitude, simulating a loosely tolerated but well corrected tokamak. While plasma symmetry is strongly broken, very weak prejudicial effects are found under these conditions. In contrast, while weak sensitivity was found for  $n=1$ , orthogonal  $n=2$  fields are found to drive rotation braking in the same co-rotating H-mode scenario, illustrating sensitivity beyond the dominant mode for higher  $n$  fields.

## 2. Description of experiment and regimes studied

This work explores orthogonal field sensitivity in a variety of plasma regimes, which are meant to provide a breath of plasma conditions for which 3D fields induce different effects. Table 1 illustrates the average global parameters of these regimes, which will now be discussed in turn.

Table 1. Global equilibrium parameters for the plasma regimes studied.

Scenario	Ohmic	Low $q_{95}$	H-mode
$I_P$ (MA)	0.8	1.4	1.2
$B_T$ (T)	1.4	1.1	1.8
$\beta_N$	0.2	0.6	2.1
$q_{95}$	4.7	2.2	4.1
$l_i$	1.5	1.0	0.9

The first regime described is a low-density Ohmic regime which is sensitive to laboratory-frame error field penetration. The ease of identification of EF penetration makes this scenario ideal for intrinsic EF measurements on DIII-D. EF penetration is known to be sensitive to the plasma density, as well as the  $n=1$  amplitude, and these are the control parameters varied in that regime. The experimental sensitivity will be a comparison of the EFCC coil current required to drive EF penetration, for applied fields that do and do not couple to the dominant mode.

The second regime is an L-mode low- $q_{95}$  scenario pursued to study MHD instabilities at low  $q_{95}$ . This plasma is sensitive to a variety of MHD instabilities[8], though application of  $n=1$  fields also drive measurable rotation braking and eventual EF penetration. Due to low  $q_{95}$ , the applied spectrum which best couples to the dominant mode has significantly different helicity than the equilibrium field.

The final regime is an ITER-similar shape H-mode scenario, where co-injected NBI yields rapid toroidal rotation. The primary sensitivity to the  $n=1$  (and  $n=2$ ) field in this regime is also rotation braking. Unlike the other scenarios, the eventual limiting instability is a born-rotating 2/1 mode. Nonetheless, prior to this event the degree of braking (thought to be due to primarily neoclassical toroidal viscosity torque) is readily measured and will be compared between different applied spectra.

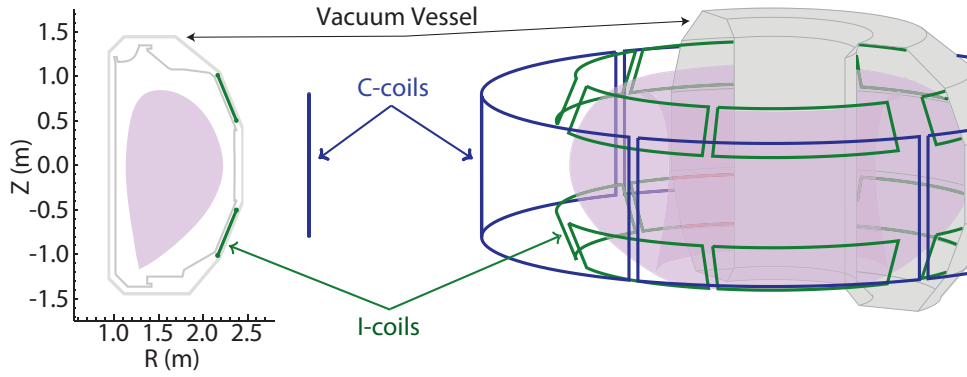


FIG. 1. Cross-section of the DIII-D vacuum vessel, typical plasma shape, and in-vessel (I) and ex-vessel (C) coils. Superpositions of in- and ex-vessel coilset fields will be used throughout this work to vary the coupling to the dominant kink mode of various plasma regimes.

### A Non-axisymmetric field setup and execution

This work is enabled by the flexible non-axisymmetric coilset in place on DIII-D, pictured in Fig. 1. Both in-vessel coils (called I-coils) and ex-vessel coils (called C-coils) are energized simultaneously to yield 3D fields with various coupling properties.

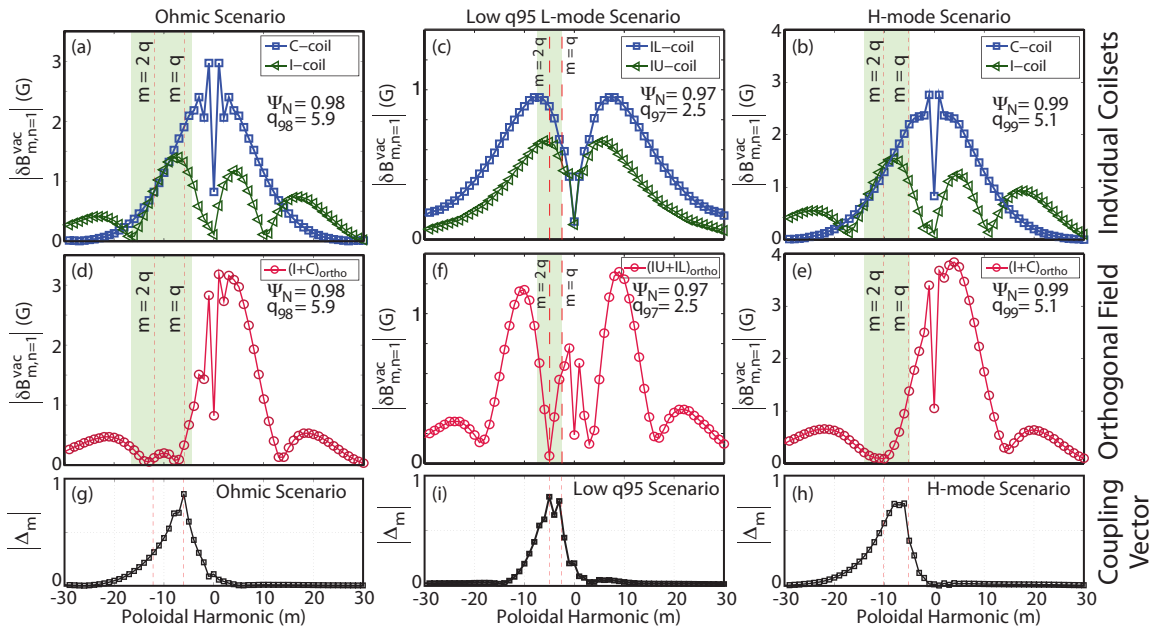


FIG. 2. Applied  $n=1$  poloidal spectra utilized for comparing plasma sensitivity in the various regimes. (a-c) illustrate poloidal spectra of the individual coilset prior to superposition. Note that in (a) and (c) the individual I-coil rows are hardwired to 240-degree upper-lower phase difference, thus acting as a single coilset. (d,e) illustrate the poloidal spectrum of the ‘orthogonal’ field. (g,h) illustrate the IPEC-produced dominant mode coupling vector for each scenario.

In each of the aforementioned scenarios, superpositions of DIII-D coilsets will be used to generate applied spectra which do or do not couple to the dominant mode. The arrangements used in each scenario are shown in Fig. 2. Individual coilset spectra, shown in Fig. 2(a-c) all have coupling, which is calculated as follows and is a scalar property of the spectrum:

$$\text{coupling} \equiv \left| \delta B_{m,n=1}^{\text{vac}} \cdot \Delta_m \right| \quad (1)$$

where  $\delta B_{m,n=1}^{vac}$  is the poloidal harmonic of the applied field and  $\Delta_m$  is the dominant mode coupling vector computed by the IPEC code[1]. Specifically, IPEC calculates the coupling from an external field to each rational surface in the plasma. A singular value decomposition (SVD) is then performed on the coupling to all rational surfaces, and the field patterns of each singular value extracted. The first left-singular vector  $\equiv \Delta_m$  represents the ‘dominant mode’ which dominates the coupling. The second left-singular vector is the sub-dominant mode, to which coupling can also be calculated. The extent to which the plasma is expected to adhere to the single dominant mode picture can be estimated by the eigenvalue separation between the dominant and sub-dominant modes, with a ten-fold separation usually found.  $\Delta_m$  is shown in Fig. 2(g,h) for the various scenarios, and calculated coupling in Table 2. Unlike the individual-coilset spectra, the orthogonal superpositions possess a spectral valley at the approximate mean value of  $\Delta_m$ , highlighted in green on Fig. 2(a-e). The location of this spectral valley is related primarily to the equilibrium  $q_{95}$ , and as such different equilibria possess spectral valleys at different poloidal mode number.

### 3. Ordering of plasma sensitivity with mode coupling

The ordering of observed plasma sensitivity in the various regimes with dominant mode coupling is presented in Fig. 3. For all investigated scenarios a strong ordering is found, and each is now described in detail.

In the low-density Ohmic regime, overwhelming experimental evidence demonstrates that the density at which EF penetration occurs is linearly related to the  $n=1$  coilset current. The experiment in this regime thus drives EF penetration at different EFCC currents and densities, and a trend-line is fit to this data. These experiments identify the locked mode density both by ramping up the EFCC current at constant density, and by ramping down the density at constant EFCC current, and both techniques are self-consistent. Figure 3(a) illustrates that for individual coilset spectra, the linear trend with EFCC current is verified, with a sensitivity of about  $0.5 \times 10^{13} \text{ cm}^{-3} / \text{ kA}$  found on DIII-D. Note that sensitivities of this nature and magnitude are what determined the original ITER physics basis geometric tolerance, prior to the discovery of additional EF sensitivities in H-mode.[5] In contrast to these well known sensitivities, the sensitivity to the orthogonal field is found to be nearly zero. Specifically, the locked mode density limit is found to be effectively unchanged despite application of large amplitude orthogonal fields. This striking result indicates that complete recovery of low density access is possible so long as the intrinsic EF’s dominant mode coupling has been nulled.

Table 2.  $n=1$  spectra coupling

Ohmic Scenario	
Spectrum	Coupling/kA
C-coil	1.92
I-coil	1.70
$(I+C)_{ortho}$	0.02
Low $q_{95}$ Scenario	
Spectrum	Coupling/kA
IL-coil	1.074
IU-coil	0.834
$(IU+IL)_{ortho}$	0.01
H-mode Scenario	
Spectrum	Coupling/kA
C-coil	1.65
I-coil	1.89
$(I+C)_{ortho}$	0.02



In the low  $q_{95}$  regime, the amount of rotation braking (measured through angular momentum degradation) is compared for a variety of toroidal phase differences between the upper and lower in-vessel coil rows (called phasing,  $\Delta\phi_{UL}$ ). While individual coilsets are different than in the previous experiment, the same principle applies and orthogonal fields are contrasted to fields which strongly couple. Comparing sequential discharges with varied upper-lower phase difference demonstrates a strong ordering of the plasma sensitivity to the dominant mode coupling. As with EF penetration in the low-density regime, the field which is computed to have no coupling drives nearly no braking.

In the co-rotating H-mode regime, rotation braking is compared for in- and ex-vessel individual coilset fields and orthogonal superpositions. Unlike in previous scenarios, some residual braking is found with the orthogonal field. However, this braking is nearly an order of magnitude reduced from that of the in-vessel coilset field alone. Thus while the co-rotating H-mode scenario still adheres to the dominant mode picture, additional sensitivities are detectable. Calculations of the neoclassical toroidal viscosity torque ( $T_{NTV}$ ) have shown that this residual braking is consistent with  $T_{NTV}$ , which is computed to originate from the low  $|m|$  components of the C-coil spectrum which are not removed when dominant mode coupling is nulled.[4, 9] However, while the residual braking is consistent with  $T_{NTV}$ , it is weak compared to the braking from the individual coilsets.

Unlike with in- and ex-vessel coilset superpositions, the symmetry of the upper and lower in-vessel coil allows simple continuous variation of the poloidal spectrum by scanning the I-coil upper-lower phase difference ( $\Delta\phi_{UL}$ ), holding the magnitude of the currents in each row constant. This technique is exploited in the low  $q_{95}$  scenario to complement the shot-to-shot comparisons shown earlier. Figure 4(a-c) shows the time-domain representation of the continuous  $\Delta\phi_{UL}$  scan, and the angular momentum ( $L_\phi$ ) is then mapped onto  $\Delta\phi_{UL}$  in (d), and compared to the instantaneous coupling in (e). Note  $\Delta\phi_{UL}$  is varied slowly (1 Hz) compared to the energy confinement time (90 ms). Good alignment of the

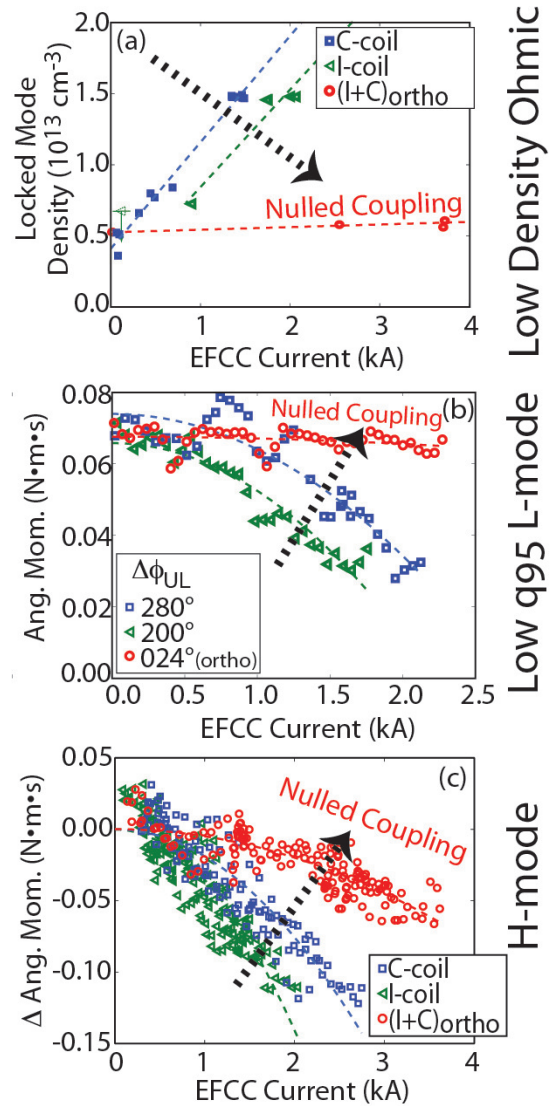


FIG. 3. Summary of  $n=1$  sensitivities as dominant-mode coupling is nulled in the various regimes. (a) Ohmic regime error field penetration, (b) Low  $q_{95}$  rotation braking, and (c) co-rotating H-mode rotation braking are all strongly reduced minimized when coupling is nulled.

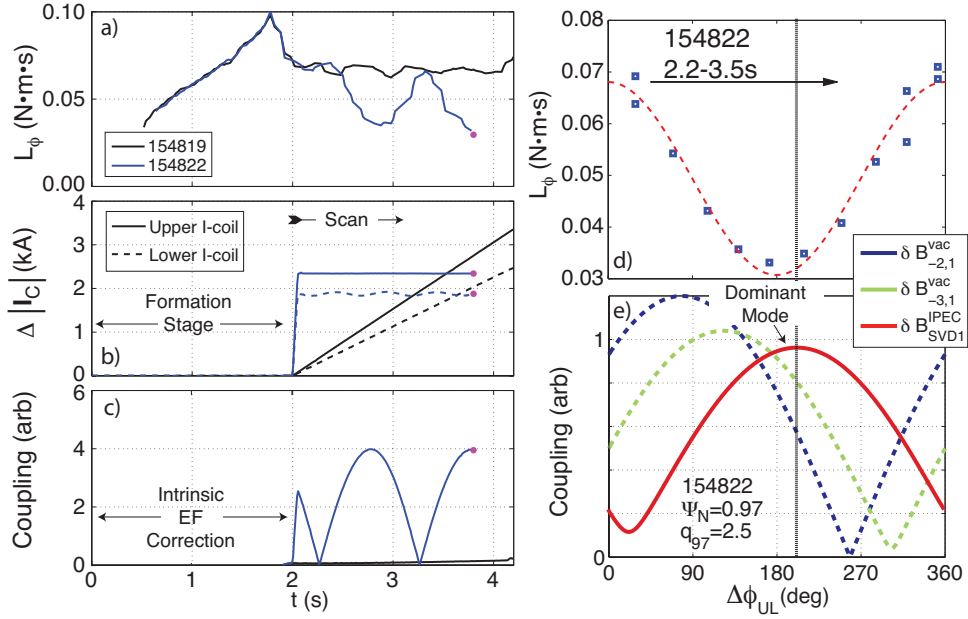


FIG. 4. (a-c) Time-domain description of the low  $q_{95}$  L-mode rotation braking experiment. A ramp of the  $(IU+IL)_{ortho}$  field (154819) does not cause rotation braking, while continuously rotating the relative phase between upper and lower I-coil rows generates a large modulation in  $L_\phi$ . When mapped to  $\Delta\phi_{UL}$ , (d) a minimum in the momentum corresponds to (e) a maximum in the coupling.

minimum in the momentum with the maximum of the dominant mode coupling is found, supporting the observations found shot-to-shot in Fig. 3. The special properties of low  $q_{95}$  coupling allows a dramatic illustration of the importance of dominant mode coupling, as opposed to simply coupling to vacuum pitch resonant components ( $m = nq$ ). This is seen in the phase shift in  $\Delta\phi_{UL}$  between maximum coupling to the dominant mode and maximum coupling to the pitch-resonant component, shown in Fig. 4(e). About a 90 degree separation is found, which is well outside the experimental error in the  $L_\phi$  minimum.

#### 4. Application to prediction of $n=1$ error field correction currents

Knowledge of dominant-mode coupling allows prediction of optimal error field correction currents based on the known geometry of the DIII-D intrinsic EF.[6] As with the creation of the orthogonal field with superpositions of individual coilsets, the process amounts to the creation of an orthogonal field with a single coilset and the intrinsic EF. Furthermore, the slowly varying shape of the coupling vector ( $\Delta_m$ ) allows approximation using a Gaussian represen-

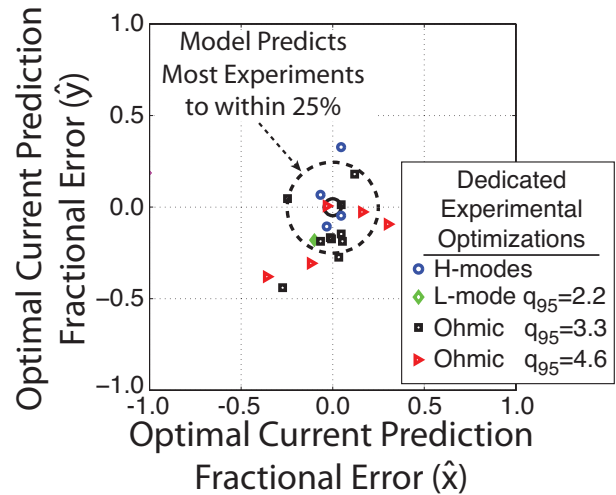


FIG. 5. Comparison of model-predicted  $n=1$  error field correction currents in comparison to experimentally determined values. The majority of over two dozen dedicated experiments conducted over a decade are found to agree within 25% with the model-predicted currents.

tation of  $\Delta_m$ , centered at a given  $m/nq$ . As seen in Fig. 2, setting the Gaussian centroid at  $m/nq = 2$  is a reasonably accurate representation of  $\Delta_m$  for the H-mode and L-mode scenario. While less accurate than a full coupling calculation, this approximation technique is powerful because it is based on equilibrium properties which are routinely calculated in real-time, thus allowing the generation of EFCC currents in real-time. The potential of this technique is shown in Fig. 5, where the approximation technique is found to be within 25% of experimentally measured optimal currents of over a broad range of conditions. This technique is currently used on DIII-D both to generate an initial guess prior to dedicated EF measurements, as well as when no EFCC measurements are planned or possible.

## 5. Extension into $n=2$ fields

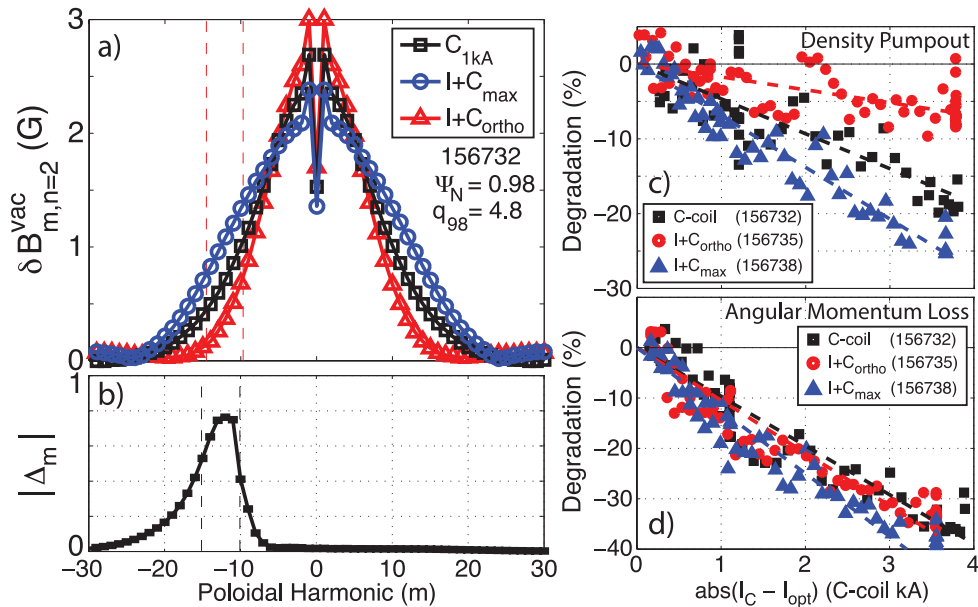


FIG. 6. Sensitivity to  $n=2$  spectra with (blue, black) and without (red) dominant mode coupling. (a-b)  $n=2$  poloidal spectrum, with and without coupling. (c) Pumpout is still strongly affected by the degree of coupling, (c) but rotation braking is found to occur regardless of coupling.

Work in the co-rotating H-mode scenario has extended study into  $n=2$  applied fields. Following the progression of the previous sections, Fig. 6(a) demonstrates the  $n=2$  poloidal spectra, while (b) shows the  $n=2$  dominant mode coupling vector ( $\Delta_m$ ) for the H-mode regime, and Table 3 presents the coupling. Ex- and in- vessel ( $\Delta\phi_{UL}=0$  hard-wiring) superpositions are used to form the orthogonal field. However, unlike  $n=1$ , now the  $\Delta_m$  is pushed to significantly higher  $|m|$ , and thus the modification of the poloidal spectrum is primarily occurring in the wings of the spectrum, leaving the majority unchanged.

Despite the minor modification to the poloidal spectrum, the difference in coupling is found to have a large effect. However, this difference is only felt in the particle transport channel, with density pumpout effectively suppressed with the orthogonal field. In

Table 3. Coupling of each  $n=2$  spectrum

Spectrum	Coupling/kA
$C_{only}$	0.417
$(I+C)_{max}$	0.848
$(I+C)_{ortho}$	0.006

contrast, both in- and ex-vessel individual coilset  $n=2$  fields are found to drive pumpout. While pumpout is again ordered by the dominant mode coupling, all cases are found to drive similar levels of magnetic braking. This is in direct contrast to results with  $n=1$ , and yields the interesting result that the orthogonal  $n=2$  field effectively decoupled the normally concurrent particle and momentum transport channels.

## 6. Concluding remarks

This work has shown that for  $n=1$  applied fields in a wide variety of plasma regimes, the plasma sensitivity to the  $n=1$  field is effectively set by the degree of coupling to a single ‘dominant’ mode of the plasma response. Equivalently,  $n=1$  fields which are specifically constructed to have no net coupling (and are thus ‘orthogonal’) to this mode are found to have very weak effects on the plasma, despite application to maximum allowable amplitude. While a robust observation for  $n=1$  fields, preliminary investigation with  $n=2$  fields suggest that the dominant mode picture is not complete for higher  $n$  fields, and additional components of the applied field need to be taken into account.

This material is based upon work supported in part by the U.S. Department of Energy, Office of Science, Office of Fusion Energy Sciences, using the DIII-D National Fusion Facility, a DOE Office of Science user facility, under Awards DE-FC02-04ER54698, DE-AC02-09CH11466, DE-FG02-04ER5471, and DE-AC05-00OR22725.

## References

- [1] J.-K. Park et al, Phys. Plasmas 14, 052110 (2007).
- [2] J.-K. Park et al, Phys. Rev. Lett. 99, 195003 (2007).
- [3] A. H. Boozer, Fusion Science and Technology 59, 561 (2011).
- [4] C. Paz-Soldan et al, Phys. Plasmas 21, 072503 (2014).
- [5] H. Reimerdes et al, Nucl. Fusion 49, 115001 (2009).
- [6] J.L. Luxon et al, Nucl. Fusion 43, 1813 (2003).
- [7] C. Paz-Soldan et al, Nucl. Fusion 54, 073013 (2014).
- [8] P. Piovesan et al, Phys. Rev. Lett. 113, 45003 (2014).
- [9] N. Logan et al, Phys. Plasmas 20 122507 (2013).